Chinese Journal of Aeronautics, (2014),27(1): 145–152

Chinese Society of Aeronautics and Astronautics
& Beihang University

Chinese Journal of Aeronautics

cja@buaa.edu.cn
www.sciencedirect.com

Sliding mode control based guidance law with impact angle constraint

Zhao Yao [a,b], Sheng Yongzhi [a,b,*], Liu Xiangdong [a,b]

[a] School of Automation, Beijing Institute of Technology, Beijing 100081, China
[b] Key Laboratory for Intelligent Control & Decision of Complex Systems, Beijing Institute of Technology, Beijing 100081, China

Received 12 January 2013; revised 19 March 2013; accepted 27 August 2013
Available online 18 December 2013

KEYWORDS

Backstepping;
Impact angle;
Sliding mode control;
Terminal guidance;
Unpowered lifting reentry vehicle

Abstract The terminal guidance problem for an unpowered lifting reentry vehicle against a stationary target is considered. In addition to attacking the target with high accuracy, the vehicle is also expected to achieve a desired impact angle. In this paper, a sliding mode control (SMC)-based guidance law is developed to satisfy the terminal angle constraint. Firstly, a specific sliding mode function is designed, and the terminal requirements can be achieved by enforcing both the sliding mode function and its derivative to zero at the end of the flight. Then, a backstepping approach is used to ensure the finite-time reaching phase of the sliding mode and the analytic expression of the control effort can be obtained. The trajectories generated by this method only depend on the initial and terminal conditions of the terminal phase and the instantaneous states of the vehicle. In order to test the performance of the proposed guidance law in practical application, numerical simulations are carried out by taking all the aerodynamic parameters into consideration. The effectiveness of the proposed guidance law is verified by the simulation results in various scenarios.

1. Introduction

For the case of the terminal guidance phase, the guidance laws are required to hit the target from a specific direction with high precision, as well as to achieve a minimal miss-distance. Traditional guidance laws, such as classical proportional navigation guidance (PNG),[1] are very popular in practical applications because of the ease of mechanization due to less information demand. Although such guidance laws can be used to attack the target accurately, they are usually silent on terminal angle constraint.

Since the concept of impact angle guidance is advanced in Ref.[2], great development has been achieved on this issue. A technique that has been commonly employed to derive such laws is using the PNG-based method. A biased PNG law is presented in Ref.[3], and the impact angle is guaranteed by adding a biased term to PNG. Similarly, in Ref.[4], an improved biased PNG law which is more simple and practical than Ref.[3] is proposed. An adaptive guidance is presented in Ref.[5], where nonlinear parameter adaptation laws are adopted in PNG to intercept a ground target. This guidance approach is effective and easy to implement. Moreover, the trajectories generated by this method are similar to the optimal trajectories. Another PNG-based guidance law, possessing the ability of intercepting a stationary target with various angles by

* Corresponding author. Tel.: +86 10 68912460.
E-mail addresses: shine3y9r@126.com (Y. Zhao), shengyongzhi@bit.edu.cn (Y. Sheng), xdliu@bit.edu.cn (X. Liu).
Peer review under responsibility of Editorial Committee of CJA.

Production and hosting by Elsevier

1000-9361 © 2014 Production and hosting by Elsevier Ltd. on behalf of CSAA & BUAA.
http://dx.doi.org/10.1016/j.cja.2013.12.011

varying the PN gains, is proposed in Ref.[6]. Afterwards, the method in Ref.[6] is further extended to deal with nonstationary nonmaneuvering targets in Ref.[7]. However, the control effort is not continuous at the instant of guidance law switching, which may increase the tracking difficulty for the flight control system.

In some recent work, the time-to-go (t_{go}) information is used to design the impact angle guidance laws. A guidance law on the basis of state dependent Riccati equation (SDRE) is proposed in Ref.[8]. The guidance problem turns to be a nonlinear regulator problem and a t_{go} based state-weighting matrix is used. A closed-form solution of a linear quadratic optimal control problem to cater for terminal angle constraint is developed in Ref.[9]. In addition, three kinds of method are introduced to calculate t_{go}. However, in practical applications, the precise estimation of t_{go} is usually a challenging work.

On the other hand, a computationally efficient technique which is called model predictive static programming (MPSP) is used to obtain impact angle constrained guidance laws. MPSP is based on nonlinear optimal control theory, and an effective trajectory optimization concept is integrated into the guidance laws. For more details, one can refer to Refs.[10,11].

Sliding mode control (SMC), as an effective method to tackle the uncertainties and disturbances, has drawn a good amount of attention from researchers around the world. In Ref.[12], a new guidance concept named intercept angle guidance is proposed. This guidance method which is implemented in the usage of sliding mode approach can be applied in three kinds of engagement scenarios, i.e., head-on, tail-chase and head-pursuit. Then, this guidance concept is further investigated in Ref.[13] with taking time-varying acceleration bounds into consideration. A novel sliding mode-based impact time and angle guidance law is presented in Ref.[14]. The line-of-sight (LOS) angle history is shaped to satisfy the needs of impact angle as well as impact time, then a backstepping based second-order sliding mode control is derived to track the pre-designed LOS angle. The method presented in Ref.[15] is a terminal SMC (TSMC)-based guidance and control law which can be used to intercept stationary, constant-velocity, and maneuvering targets with any impact angle, even under the circumstance of large initial heading errors. In spite of the effectiveness of the proposed method from the constant-velocity missile point of view, it is difficult to estimate its performance by taking all the aerodynamic parameters into consideration. In Ref.[16], a scheme of integrated guidance and control on the basis of an adaptive SMC algorithm is developed. In this work, the nonlinear dynamics is taken into account, and the robust characteristics of the algorithm are validated in the case of aerodynamic parameter perturbation; however, the range of available terminal angle is limited.

In this paper, an SMC-based guidance law is developed to hit a stationary target from a specified direction with high precision. The nonlinear point-mass dynamics in the pitch plane is used to evaluate the guidance law. As the sliding mode function is specially designed according to the terminal constraints, the associated sliding mode is established to guarantee the interception with the specified impact angle where the backstepping approach is utilized. Moreover, the closed-loop dynamics is insensitive to uncertainties and disturbances by the virtue of the strong robustness of SMC. The guidance law features in four characteristics. Firstly, aerodynamic characteristics are taken into account in the design of the proposed guidance law. As a result, the simulation results obtained from this method tally well with the actual situation. Secondly, there is a wide range of achievable impact angle in the usage of the guidance law. It guarantees the capability of the proposed guidance law to meet different mission requirements. Thirdly, the guidance scheme is quite robust to initial conditions as well as parameter perturbation. Finally, the guidance command is very smooth and it can be easily realized by the attitude control system.

2. Problem formulation

In this paper, a two-dimensional homing scenario is considered. To make it explicit, the engagement geometry in inertial coordinate frame is shown in Fig. 1. The missile and the target are represented by M and T; the missile's acceleration is denoted by u; the velocity and flight path angle of the missile are defined as V and γ respectively, with V_f and γ_f being their final values. In addition, the missile mass is represented by m and the gravity acceleration $g = 9.81$ m/s is treated as a constant.

The equations of motion in the terminal guidance phase can be given as

$$\dot{x} = V\cos\gamma \tag{1}$$

$$\dot{y} = V\sin\gamma \tag{2}$$

$$\dot{V} = -\frac{D}{m} - g\sin\gamma \tag{3}$$

$$\dot{\gamma} = \frac{L}{mV} - \frac{g\cos\gamma}{V} \tag{4}$$

where the position coordinates are x and y. The terms L and D are the aerodynamic lift and drag which are defined by

$$L = qSC_L \tag{5}$$

$$D = qSC_D \tag{6}$$

where $q = 0.5\rho V^2$ is the dynamic pressure which is dependent on the air density ρ and the velocity V; S is the reference area of the vehicle; the terms C_L and C_D are the lift and drag coefficients that are dependent on the angle of attack α and Mach number Ma.

Time t is taken as the independent variable in the equations of motion (1)–(4). However, the flight time of the terminal guidance phase is usually not the key question we are concerned about. In Ref.[17], the downrange x is used as the independent variable to land the reusable launch vehicle

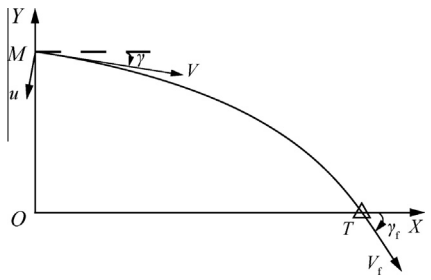

Fig. 1 Engagement geometry.

(RLV) at a given downrange location. Although it has an advantage in dealing with such landing problems, it is not appropriate for the impact angle constrained situations. This is because each independent variable only possesses one corresponding dependent variable. If the desired impact angle is set to be less than $-90°$, each x will have two corresponding y when the value of x is larger than its final value. As a consequence, the desired impact angles which are less than $-90°$ are not achievable. Therefore, a new independent variable is needed to handle such problems.

The perceived wisdom is using the altitude as the independent variable instead of the downrange. Because the altitude of the reentry vehicle is usually monotonically decreasing during the terminal phase, each altitude has only one corresponding downrange. Note that the independent variable used in the simulation requires a monotonically increasing format. Therefore, a new variable $Y = y_0 - y$ is taken as the independent variable of the above system instead of t, where y_0 is the initial altitude of the vehicle. Thus, the system model can be changed to the following equations:

$$x' = \frac{\mathrm{d}x}{\mathrm{d}Y} = -\cot\gamma \tag{7}$$

$$y' = \frac{\mathrm{d}y}{\mathrm{d}Y} = -1 \tag{8}$$

$$V' = \frac{\mathrm{d}V}{\mathrm{d}Y} = \frac{D + mg\sin\gamma}{mV\sin\gamma} \tag{9}$$

$$\gamma' = \frac{\mathrm{d}\gamma}{\mathrm{d}Y} = -\frac{L - mg\cos\gamma}{mV^2\sin\gamma} \tag{10}$$

The time becomes an incidental variable given by

$$t' = \frac{\mathrm{d}t}{\mathrm{d}Y} = -\frac{1}{V\sin\gamma} \tag{11}$$

This new model is used to develop the guidance law detailed in the next section, and the derivative of the flight path angle, γ', is considered as the control input.

3. Impact angle guidance law design

In this section, an SMC-based guidance law is designed, which results in very good accuracy both in miss distance and impact angle constraint.

The target's position is given as $(x_\mathrm{f}, y_\mathrm{f})$ and the required impact angle is set to be γ_f, and the subscript "f" represents the final value of the variable. Since y_f is also the final altitude of the vehicle, we have $Y_\mathrm{f} = y_0 - y_\mathrm{f}$. The objective is to enforce x and γ to x_f and γ_f respectively as Y reaches Y_f. An interesting result can be obtained from Eq. (7) that x' only relates to γ, which means if the desired impact angle is given, the final value of x' is also determined. As a consequence, the impact angle guidance problem can be solved by controlling the final value of x'.

Motivated by this idea, the sliding function is designed as follows:

$$S_1 = x - x_\mathrm{f} - x'_\mathrm{f}(Y - Y_\mathrm{f}) \tag{12}$$

Differentiating S_1 with respect to Y yields

$$S'_1 = x' - x'_\mathrm{f} \tag{13}$$

It is obvious that at the time of interception, the value of $Y - Y_\mathrm{f}$ will go to zero. Therefore, if S_1 and S'_1 also go to zero at the same time, the miss-distance will be minimized and the impact angle constraint will be satisfied. To make the first appearance of the control effort γ', the second derivative of S_1 is taken and one gets

$$S''_1 = x'' = \frac{1}{\sin^2\gamma}\gamma' \tag{14}$$

So the sliding function S_1 has a relative degree of two.

In Ref.[18], a novel second-order sliding mode method based on an adaptive backstepping approach is derived. This method can be used to ensure that both S and S' do not come to zero until t reaches t_f. On the basis of this idea, a similar approach is developed which is able to guarantee $S = S' = 0$ to come into existence at $Y = Y_\mathrm{f}$ instead of $t = t_\mathrm{f}$.

Theorem 1. Consider the sliding mode function S_1. If S'_1 is treated as a control input which takes the form of

$$S'_1 = -\frac{nS_1}{Y_\mathrm{f} - Y}, \qquad n > 1 \tag{15}$$

both S_1 as well as its derivative S'_1 will go to zero at $Y = Y_\mathrm{f}$.

Proof. From Eq. (15), one gets

$$S'_1 = \frac{\mathrm{d}S_1}{\mathrm{d}Y} = -\frac{nS_1}{Y_\mathrm{f} - Y} \tag{16}$$

Rearranging variables, Eq. (16) can be rewritten as

$$\frac{1}{S_1}\mathrm{d}S_1 = -n\frac{1}{Y_\mathrm{f} - Y}\mathrm{d}Y \tag{17}$$

Assuming the initial state of Eq. (17) is $(Y_\mathrm{b}, S_{1\mathrm{b}})$. Then, integrating Eq. (17) from $(Y_\mathrm{b}, S_{1\mathrm{b}})$ to the later point (Y, S_1), we have

$$\int_{S_{1\mathrm{b}}}^{S_1}\frac{1}{S_1}\mathrm{d}S_1 = -n\int_{Y_\mathrm{b}}^{Y}\frac{1}{Y_\mathrm{f} - Y}\mathrm{d}Y \tag{18}$$

Thus, the following equation can be obtained

$$\ln\frac{S_1}{S_{1\mathrm{b}}} = \ln\frac{(Y_\mathrm{f} - Y)^n}{(Y_\mathrm{f} - Y_\mathrm{b})^n} \tag{19}$$

Taking the exponential of both sides of Eq. (19), the analytical expression for S_1 can be found as

$$S_1 = \frac{S_{1\mathrm{b}}}{(Y_\mathrm{f} - Y_\mathrm{b})^n}(Y_\mathrm{f} - Y)^n \tag{20}$$

Differentiating Eq. (20) with respect to Y yields

$$S'_1 = -\frac{nS_{1\mathrm{b}}}{(Y_\mathrm{f} - Y_\mathrm{b})^n}(Y_\mathrm{f} - Y)^{n-1} \tag{21}$$

From Eqs. (20) and (21), we can conclude that S_1 and S'_1 will both go to zero at $Y = Y_\mathrm{f}$ as long as the value of n is larger than one. □

Therefore, the desired trajectory S'_1 is defined by Eq. (15), and we only need to make it happen. That is to say, a control input γ' needs to be derived to enforce S'_1 to approach and then stay on the desired trajectory.

A new sliding function is defined as

$$S_2 = S_1' + \frac{nS_1}{Y_f - Y}, \qquad n > 1 \tag{22}$$

The derivative of S_2 can be obtained as

$$S_2' = S_1'' + \frac{nS_1'(Y_f - Y) + nS_1}{(Y_f - Y)^2}, \qquad n > 1 \tag{23}$$

For clarity, let $M = \frac{nS_1'(Y_f - Y) + nS_1}{(Y_f - Y)^2}$, we have

$$S_2' = \frac{1}{\sin^2\gamma}\gamma' + M \tag{24}$$

Next, the Lyapunov theory will be used to obtain the control input.

Define the following positive definite Lyapunov function as

$$V_1 = \frac{1}{2}S_2^2 \tag{25}$$

Differentiating V_1 with respect to Y yields

$$V_1' = S_2 S_2' = S_2\left(\frac{1}{\sin^2\gamma}\gamma' + M\right) \tag{26}$$

The control input, γ', takes the form of

$$\gamma' = \gamma'_{eq} + \gamma'_{dis} \tag{27}$$

where γ'_{eq} is the equivalent control input which guarantees $S_2' = 0$ for the nominal model, and γ'_{dis} is the discontinuous switching control input which ensures the attractability of the sliding surface.

The equivalent control input is selected as

$$\gamma'_{eq} = -M\sin^2\gamma \tag{28}$$

Substituting Eq. (28) into Eq. (27) and the result is substituted into Eq. (26), which yields

$$V_1' = S_2\left(\frac{1}{\sin^2\gamma}\gamma'_{dis}\right) \tag{29}$$

Then, the discontinuous control effort is chosen as

$$\gamma'_{dis} = -k\sin^2\gamma \,\mathrm{sgn}\, S_2, \qquad k > 0 \tag{30}$$

which, on substitution in Eq. (29), yields

$$V_1' = -k|S_2| \tag{31}$$

If $S_2 \neq 0$, from $k > 0$, one has $V_1' < 0$, according to Lyapunov stability principle, the conclusion that the system is asymptotic stable can be drawn. In addition, because the system must perform some movement along the trajectory of Eq. (15) to satisfy the terminal constraints, the sliding motion should be established before $Y = Y_f$.

Substituting Eqs. (28), (30) into Eq. (27) and the result is substituted into Eq. (24), one gets

$$S_2' = -k\mathrm{sgn}S_2 \tag{32}$$

From Eq. (32), we can conclude that k denotes the speed of approaching the sliding surface $S_2 = 0$. Therefore, the switching gain k can be calculated by

$$k = \frac{|S_2(0)|}{Y_b}, \quad Y_b = pY_f, \qquad 0 < p < 1 \tag{33}$$

where $S_2(0)$ is the initial value of S_2. In this way, the sliding mode S_2 will reach zero at $Y = Y_b$ and keep staying on the sliding surface thereafter.

Till now, the final expression of the control effort γ' can be given as

$$\gamma' = -\left[\frac{nS_1'(Y_f - Y) + nS_1}{(Y_f - Y)^2} + \frac{|S_2(0)|}{pY_f}\mathrm{sgn}S_2\right]\sin^2\gamma \tag{34}$$

It should be noted that the guidance process is over at the instance the value of Y reaches Y_f. In other words, no movement is allowed along the trajectory of $S_1 = 0$. Therefore, under the circumstances of hitting a stationary ground-based target, the available range of γ_f is $(-\pi, 0)$. The reason of excluding 0 and π from the range is that the values of cot(0) and cot($-\pi$) do not exist.

Since the control effort will enforce the system states on the sliding surface $S_2 = 0$ for a certain period of time, the inherent chattering problem of SMC would likely to be experienced. To solve this problem, a simple saturation function $\mathrm{sgmf}(S) = \frac{S}{|S| + \varepsilon}$ could be used instead of the sign function, where ε is the boundary layer. In this way, the system is no longer asymptotic but could only converge to a boundary layer about the sliding surface. However, by setting the size of the boundary layer adequately small, the error can be limited within a negligible range.

In many scenarios, the desired control effort for a lifting reentry vehicle is the angle of attack α, not the derivative of the flight path angle γ'. However, if the instantaneous value of γ' is given, the angle of attack can be obtained. Substituting the control input γ' into Eq. (10), the lift L can be found as

$$L = mg\cos\gamma - mV^2\gamma'\sin\gamma \tag{35}$$

Then from Eq. (5) and Eq. (35), the lift coefficient C_L can then be obtained as

$$C_L = \frac{L}{qS} = \frac{mg\cos\gamma - mV^2\gamma'\sin\gamma}{qS} \tag{36}$$

As long as C_L is achieved, the associated angle of attack can be easily derived using numerical methods such as Newton's method and linear interpolation.

4. Simulation results

In order to verify the effectiveness of the SMC-based impact angle guidance law advanced in the previous section, numerical simulations for different situations are presented in this section.

In the simulations, a hypothetical hypersonic lifting reentry vehicle of 1000 kg in weight and 2.5 m^2 in reference area is used to hit a stationary ground-based target. The aerodynamic model of the vehicle is given as follows:

$$C_L = C_{L0} + C_{L\alpha}\alpha \tag{37}$$

$$C_D = C_{D0} + KC_L^2 \tag{38}$$

The values of the parameters used in Eqs. (37) and (38) are given below

$$C_{L0} = \frac{1}{20\pi}\arctan(10Ma - 10) - 0.035 \tag{39}$$

$$C_{L\alpha} = 0.057\mathrm{e}^{-0.654Ma} + 0.014 \tag{40}$$

Table 1 Zero-lift drag coefficient with Ma.

Ma	C_{D0}	Ma	C_{D0}
0	0.0075	5	0.0092
0.5	0.0075	5.5	0.0087
1	0.0105	6	0.0082
1.5	0.0160	6.5	0.0080
2	0.0133	7	0.0078
2.5	0.0128	7.5	0.0079
3	0.0125	8	0.0080
3.5	0.0115	8.5	0.0080
4	0.0110	9	0.0080
4.5	0.0099	9.5	0.0080

$$K = 1.85\left(1 - \mathrm{e}^{-0.2356Ma}\right) \tag{41}$$

The zero-lift drag coefficient C_{D0} can be obtained by linear interpolation among the data in Table 1 with Mach number as the independent variable.

The atmospheric properties used in the simulations are based on the 1976 US Standard Atmosphere. During the implementation, the actual control effort α is bounded within $(-30°, +30°)$. First of all, the wide capture range of the proposed guidance law is testified by the simulations with different impact angles. Then, some cases are put forward on the basis of vertical impact. Subsequently, the simulation results with fifth-order system delay are demonstrated. Finally, Monte Carlo simulations are presented to validate the robustness of the guidance law. The miss distance and the impact angle error are defined as the absolute values that the final position and terminal flight path angle deviate from their desired values.

4.1. Simulations with different impact angles

The simulation parameters for this case are listed in Table 2. The flight trajectories, flight path angle histories and angle of attack profiles for this case are plotted in Fig. 2(a)–(c), respectively. The results show that the proposed guidance law possesses a wide capture range of impact angles. Fig. 2(c) shows that control saturation phenomenon occurs during the process of achieving the design goal of $-150°$ and $-170°$. This is because a high value of control effort is necessary to ensure the vehicle to maneuver to achieve such impact angle requirements. Besides, the miss distances as well as impact angle errors are listed in Table 3. The miss distances are all limited within 10^{-4} m and the impact angle errors are no bigger than

Table 2 Simulation parameters for cases of different impact angles.

Parameter	Value	Parameter	Value
x_0 (km)	0	y_f (km)	0
y_0 (km)	20	γ_f (°)	-10, -30, -90, -150, -170
V_0 (m/s)	1700	n	4
γ_0 (°)	-10	ε	10^{-3}
x_f (km)	60	p	0.3

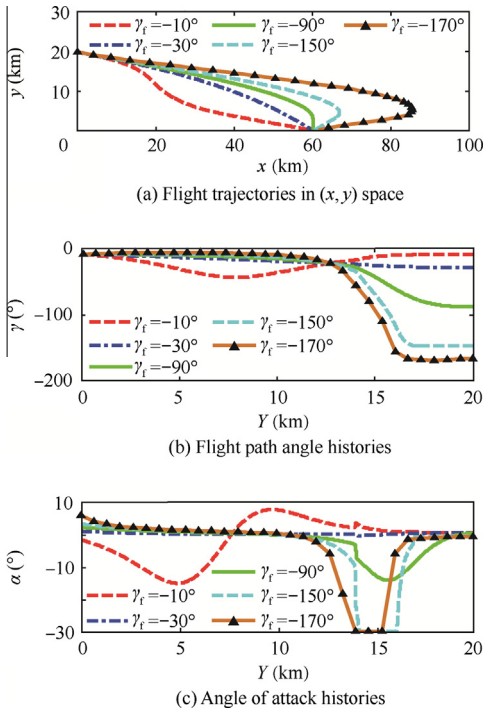

Fig. 2 Simulation results with different impact angles.

Table 3 Miss distances and impact angle errors.

Desired impact angle (°)	Miss distance (m)	Impact angle error (°)
-10	1.0262×10^{-5}	3.0327×10^{-6}
-30	1.9299×10^{-5}	3.5163×10^{-6}
-90	7.2760×10^{-11}	2.1587×10^{-11}
-150	1.8934×10^{-5}	2.4075×10^{-6}
-170	8.0306×10^{-6}	5.1661×10^{-6}

10^{-5}(°). The results show excellent performance of the proposed guidance law against different impact angle constraints.

4.2. Vertical impact cases

In this part, different scenarios of vertical impact case are presented. In all these simulations, if not stated, the miss distances are limited within 10^{-3} m and the corresponding impact angle errors are less than 10^{-4}(°). Additionally, the parameters used in the following cases, unless specified, are the same as in Table 4.

(1) Case A: A general vertical impact case.

In this case, a general vertical impact case is presented in Fig. 3(a)–(g). The vehicle's flight trajectory and control effort profile are plotted in Fig. 3 (a) and (d), respectively. For most of the time, the angle of attack changes slowly. However, it decreases quickly during the final period of the flight to achieve the desired impact angle. As the flight path angle is nearly achieved, it will converge to the zero-lift angle of attack. As a consequence, the altitude of the vehicle changes gradually for the early period of the flight but it descends fast when it gets close to the target. It can be seen in Fig. 3(e) that the

Table 4 Simulation parameters for vertical impact cases.

Parameter	Value	Parameter	Value
x_0 (km)	0	y_f (km)	0
y_0 (km)	20	γ_f (°)	−90
V_0 (m/s)	1700	n	4
γ_0 (°)	−3	ε	10^{-3}
α_0 (°)	3	p	0.3
x_f (km)	100		

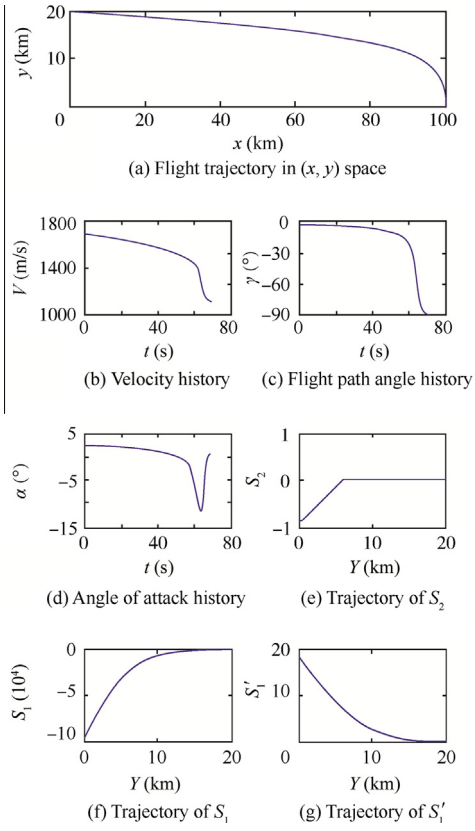

Fig. 3 Simulation results of general vertical impact case.

sliding mode S_2 occurs at the instant of $Y = 0.3Y_f$. From then on, the system states stay on the trajectory of $S_2 = 0$, which guarantees the occurrence of $S_1 = 0$ and $S_1' = 0$ at the final time (see Fig. 3(f) and (g)). It can be drawn from Fig. 3(b) and (c) that the impact angle requirement is satisfied and the velocity history is satisfactory.

(2) Case B: Vertical impact with different n.

In this case, the performance of the proposed guidance law with respect to different n is tested and the associated results are shown in Fig. 4(a)–(f). The values of n in the simulations are selected as 2, 3 and 4, respectively. It can be concluded from Fig. 4 (b) and (f) that the variety of n does not have much effect on the velocity histories. However, the trajectories of S_1

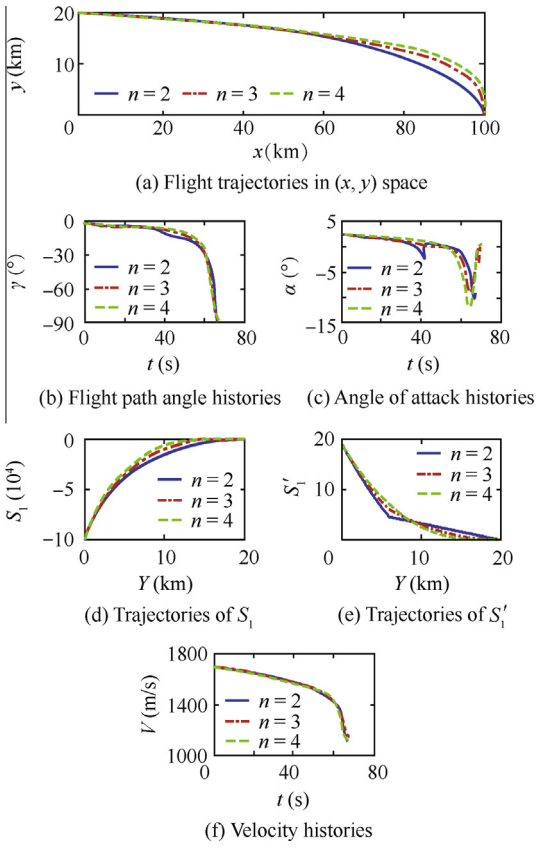

Fig. 4 Simulation results of vertical impact case with different n.

and S_1' as well as the flight path angle histories are influenced apparently by the variety of n. It is because the behaviors of S_1 and S_1' are determined by the value of n.

From Eqs. (25) and (26), we can see that the value of n determines the shape of the trajectories of S_1 and S_1'. For instance, if $n = 2$ is selected, the trajectories of S_1 and S_1' are parabola and straight line, respectively. Note, from Fig. 4(d) and (e), that the solid lines are the trajectories of S_1 and S_1' when n is set to 2. After $Y = Y_b$, Eq. (15) is satisfied, and thus the two trajectories turn out to be parabola and straight line respectively. In addition, it can be drawn from Eq. (13) that the trajectory of S_1' can affect the behavior of the flight path angle directly. As the value of n increases, the trajectory of S_1' tends to be zero more quickly, so the flight path angle converges to its desired value faster. As a consequence, less time is needed for the vehicle to change its course to achieve the terminal angle requirement (see Fig. 4 (a)). In Fig. 4(c), it appears that the angle of attack histories are smoother and their peak values become larger as the value of n increases.

(3) Case C: Vertical impact with different p.

This set of simulations involves implementing the guidance law with different p. The simulation results are described in Fig. 5(a)–(f). The values of p are chosen as 0.3, 0.5 and 0.7, respectively. It can be seen from Fig. 5(f) that the sliding mode occurs at the desired position for each value of p. From the simulation results, it is obvious that varying the value of p does not affect the performance of the proposed guidance law apparently. Similar to the previous cases, the guidance law is able to steer the

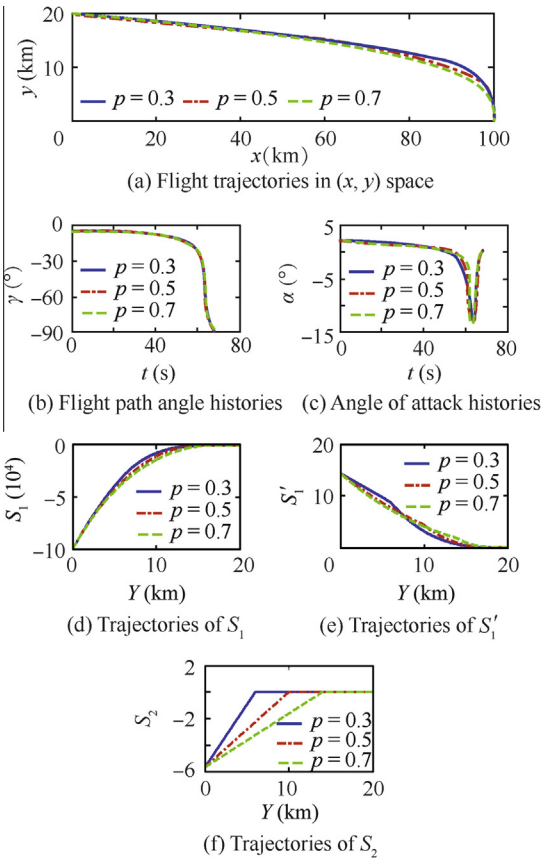

Fig. 5 Simulation results of vertical impact case with different p.

vehicle to attack the target with the desired terminal angle (see Fig. 5(a) and (b)). It can be noticed from Fig. 5(c) that a larger magnitude of α is needed for a larger value of p.

(4) Case D: Simulations with fifth-order system delays.

In order to verify the performance of the proposed guidance law in practical application, the simulations in this part are carried out with fifth-order system delays. The reason for choosing fifth-order lag is to make a clear description of the lag model. In this canonic model, one time constant represents the seeker, another represents the noise filter, and the three time constants represent the flight-control system.[19] The fifth-lag guidance system possesses the following transfer function

$$\frac{\alpha_r}{\alpha_c} = \frac{1}{(\tau s + 1)^5} \tag{42}$$

where τ is the guidance system time constant, and α_c and α_r are the required command and the realized command, respectively. The time constant τ is set to be 0.1s. Other parameters used in this case are the same as Table 2.

Fig. 6(a) and (b) show that the vehicle is able to hit the target with the desired impact angle even under high-order time delays. It can be seen from Fig. 6(c) that the time histories of the required command and the realized command are very close to each other. This means that the control effort obtained from the proposed guidance law can be easily implemented in practical applications. The simulation results prove the robustness of the proposed guidance law with respect to high-order system delays.

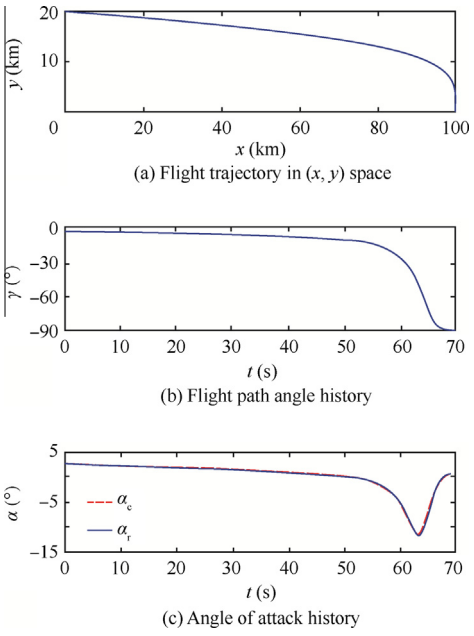

Fig. 6 Simulation results of vertical impact case with fifth-order delays.

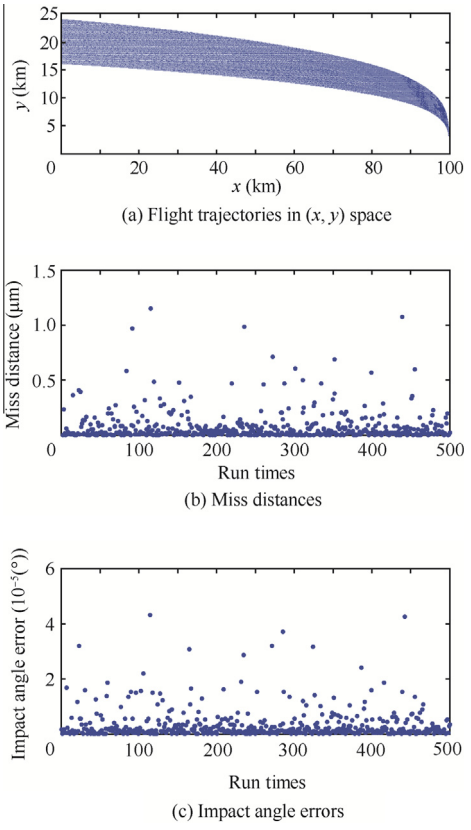

Fig. 7 Monte Carlo simulation results.

(5) Case E: Monte Carlo simulations.

In the previous cases, each simulation focuses on one situation. In this case, many different situations as well as

high-order system delays are taken into consideration in one simulation. Initial perturbation in state parameters such as altitude, velocity and flight path angle is generated randomly in uniform distribution. The range of dispersion is $\pm 20\%$. Besides, aerodynamic modeling error is applied as variation in ρ within a range of $\pm 20\%$. What's more, random noise ranging between -5% and 5% of the nominal value of ρ is added to the aerodynamic model. The Monte Carlo simulation for 500 runs is presented in Fig. 7. From Fig. 7(a), we can see that due to the initial perturbation in state parameters, the flight trajectories are apparently different from each other. However, all of them converge to one point at the end of the flight. Fig. 7(b) and (c) show that the results are equally good even under such severe conditions. For majority of the cases, the miss distances and the impact angle errors are very close to zero. The miss distances in all cases are limited in 1.2×10^{-6} m, while the impact angle errors are no bigger than $5 \times 10^{-5}(^\circ)$. Good robustness of the proposed guidance law can be concluded from the simulation results.

5. Conclusion

An SMC-based guidance law with terminal angle constraint for unpowered lifting reentry vehicles has been proposed in this paper. A special sliding mode function is designed on the basis of terminal constraints. A backstepping approach is used to obtain the control effort which could enforce the sliding mode function together with its derivative to zero at the time of interception. The guidance approach is characterized by its simple format and less information requirement. The accuracy of the guidance law has been demonstrated in the planar engagement scenario with considering aerodynamic characteristics. A wide range of impact angle has been validated. In addition, different simulation parameters are adopted to verify the robustness of the proposed guidance law. Moreover, the performance of the proposed method is testified by implementing the guidance law with respect to high-order system delays. Finally, strong robustness of the guidance law has been drawn from the Monte Carlo simulations. The future work may include the extension to three-dimensional engagement scenarios and the trajectory shaping ability.

Acknowledgements

This study was co-supported by National Natural Science Foundation of China (No. 61104153) and National Basic Research Program of China (No. 2012CB720000).

References

1. Siouris GM. *Missile guidance and control systems*. New York: Springer; 2003, p. 194–225.
2. Kim M, Grider KV. Terminal guidance for impact attitude angle constrained flight trajectories. *IEEE Trans Aerosp Electron Syst* 1973;**9**(6):852–9.
3. Kim BS, Lee JG, Han HS. Biased PNG law for impact with angular constraint. *IEEE Trans Aerosp Electron Syst* 1998;**34**(1):277–88.
4. Jeong SK, Cho SJ, Kim EG. Angle constraint biased PNG. In: *Proceedings of 5th Asian Control Conference*; 2004. p. 1849–54.
5. Lu P, Doman DB, Schierman JD. Adaptive terminal guidance for hypervelocity impact in specified direction. *J Guid Control Dyn* 2006;**29**(2):269–78.
6. Ratnoo A, Ghose D. Impact angle constrained interception of stationary targets. *J Guid Control Dyn* 2008;**31**(6):1816–21.
7. Ratnoo A, Ghose D. Impact angle constrained guidance against nonstationary nonmaneuvering targets. *J Guid Control Dyn* 2010;**33**(1):269–75.
8. Ratnoo A, Ghose D. State dependent Riccati equation based guidance law for impact-angle-constrained trajectories. *J Guid Control Dyn* 2009;**32**(1):320–6.
9. Ryoo CK, Cho H, Tahk MJ. Optimal guidance laws with terminal impact angle constraint. *J Guid Control Dyn* 2005;**28**(4):724–32.
10. Dwivedi PN, Bhattacharya A, Padhi R. Suboptimal midcourse guidance of interceptors for high speed targets with alignment angle constraint. *J Guid Control Dyn* 2011;**34**(3):860–77.
11. Oza HB, Padhi R. Impact-angle-constrained suboptimal model predictive static programming guidance of air-to-ground missiles. *J Guid Control Dyn* 2012;**35**(1):153–64.
12. Shima T. Intercept-angle guidance. *J Guidance Control Dyn* 2011;**34**(2):484–92.
13. Taub I, Shima T. Intercept angle missile guidance under time-varying acceleration bounds. 2012. Report No. AIAA-2012-4472.
14. Harl N, Balakrishnan SN. Impact time and angle guidance with sliding mode control. *IEEE Trans Control Syst Technol* 2012;**20**(6):1436–49.
15. Kumar SR, Rao S, Ghose D. Sliding-mode guidance and control for all-aspect interceptors with terminal angle constraints. *J Guid Control Dyn* 2012;**35**(4):1230–46.
16. Hou MZ, Duan GR. Integrated guidance and control of homing missiles against ground fixed targets. *Chin J Aeronaut* 2008;**21**(2):162–8.
17. Heydari A, Balakrishnan SN. Optimal online path planning for approach and landing guidance. 2011. Report No.: AIAA-2011-6641.
18. Harl N, Balakrishnan SN. Reentry terminal guidance through sliding mode control. *J Guid Control Dyn* 2010;**33**(1):186–99.
19. Zarchan P. *Tactical and strategic missile guidance*. 4th ed. New York: AIAA Inc.; 2002, p. 95–118.

Zhao Yao received the B.S. degree from University of Electronic Science and Technology of China (UESTC) in 2010. He is now pursing the Ph.D. in Beijing Institute of Technology (BIT). His research interests include guidance and control, trajectory planning and optimization.

Sheng Yongzhi received the B.S. and M.S. degrees from Beihang University in 2003 and 2006, respectively, and then received his Ph.D. degree from the Graduate School of the Second Academy of China Aerospace in 2009. From 2009 to 2011 he did his postdoctoral research in Beihang University. He is currently a lecturer with School of Automation in Beijing Institute of Technology (BIT). His research interests include guidance of reentry vehicle.

Liu Xiangdong received M.S. and Ph.D. degrees from Harbin Institute of Technology (HIT) in 1992 and 1995, respectively. From 1998 to 2000, he did his postdoctoral research in Mechanical Postdoctoral Research Center in HIT. He is currently a professor with School of Automation in Beijing Institute of Technology (BIT). His research interests include high-precision servo control, spacecraft attitude control, Chaos theory.